

Bis(permethyindenyl) Complexes of Thorium: Synthesis, Structure, and Reactivity

Tina M. Trnka, Jeffrey B. Bonanno, Brian M. Bridgewater, and Gerard Parkin*

Department of Chemistry, Columbia University, New York, New York 10027

Received March 26, 2001

A variety of thorium complexes incorporating the bulky permethyindenyl ligand (Ind* = C₉Me₇) have been synthesized and characterized. Specifically, the dichloride Ind*₂ThCl₂ is obtained by reaction of ThCl₄ with Ind*Li, from which Ind*₂ThMe₂, Ind*₂Th(NMe₂)₂, Ind*₂Th(NC₄H₄)₂, and Ind*₂Th(η³-H₃BH)₂ may be obtained by metathesis with MeLi, LiNMe₂, LiNC₄H₄, and Ca(BH₄)₂, respectively. In contrast to simple metathesis, reaction of Ind*₂ThCl₂ with KN(SiMe₃)₂ yields the metallacycle Ind*₂Th(η²-CH₂SiMe₂NSiMe₃). X-ray diffraction studies on Ind*₂ThCl₂, Ind*₂ThCl(μ-Cl)₂Li(tmeda), Ind*₂ThMe₂, Ind*₂Th(NMe₂)₂, Ind*₂Th(η²-CH₂SiMe₂NSiMe₃), and Ind*₂Th(η³-H₃BH)₂ indicate that the permethyindenyl ligands in these complexes exhibit a variety of conformations.

Introduction

During the past two decades, there has been considerable interest in using substitutes for the ubiquitous cyclopentadienyl ligand in order to enhance or change the reactivity of organometallic complexes. Modifications of the cyclopentadienyl ligand have involved: (i) the use of bulky substituents to enforce the formation of mononuclear species with reactive functionalities,^{1,2} (ii) incorporation of *ansa* bridges between two cyclopentadienyl rings to displace the cyclopentadienyl ligands from their natural positions and thereby modulate the reactivity of a metal center,³ (iii) the use of donor substituents to provide a chelating ligand,⁴ and (iv) application of indenyl, fluorenyl, and other fused-ring derivatives.^{5,6} Although each of these modifications can have a profound effect on the chemistry of the system

under consideration, the influence of indenyl ligands is sufficiently pronounced that it has been ascribed the term "indenyl effect".^{6,7} The majority of studies have focused on the parent indenyl ligand, Ind = C₉H₇, but the permethyindenyl ligand (Ind* = C₉Me₇)⁸ has been introduced with the notion that permethylation may exert effects in indenyl chemistry similar to those observed for cyclopentadienyl complexes.

In contrast to the parent indenyl ligand, there are presently relatively few applications of its permethylated counterpart in organometallic chemistry. Permethyindenyl complexes are, nevertheless, known for titanium,⁹ chromium,¹⁰ iron,^{11,12} cobalt,^{10–12} zirconium,¹³ molybdenum,¹⁴ rhenium,¹⁵ rhodium,^{7b,16–20} lanthanum,²¹ neodymium,²¹ erbium,²¹ thorium,²² and ura-

(1) For reviews of the application of heavily substituted cyclopentadienyl ligands, see: (a) Janiak, C.; Schumann, H. *Adv. Organomet. Chem.* **1991**, *33*, 291–393. (b) Okuda, J. *Top. Curr. Chem.* **1991**, *160*, 97–145.

(2) For example, permethylation afforded the first methylene-hydride complex, Cp*₂Ta(CH₂)H. See: van Asselt, A.; Burger, B. J.; Gibson, V. C.; Bercaw, J. E. *J. Am. Chem. Soc.* **1986**, *108*, 5347–5349.

(3) (a) Green, J. C. *Chem. Soc. Rev.* **1998**, *27*, 263–271. (b) Conway, S. L. J.; Dijkstra, T.; Doerrer, L. H.; Green, J. C.; Green, M. L. H.; Stephens, A. H. H. *J. Chem. Soc., Dalton Trans.* **1998**, 2689–2695. (c) Labella, L.; Chernega, A.; Green, M. L. H. *J. Chem. Soc., Dalton Trans.* **1995**, 395–402. (d) Churchill, D.; Shin, J. H.; Hascall, T.; Hahn, J. M.; Bridgewater, B. M.; Parkin, G. *Organometallics* **1999**, *18*, 2403–2406. (e) Chernega, A.; Cook, J.; Green, M. L. H.; Labella, L.; Simpson, S. J.; Souter, J.; Stephens, A. H. H. *J. Chem. Soc., Dalton Trans.* **1997**, 3225–3243. (f) Churchill, D. G.; Bridgewater, B. M.; Parkin, G. *J. Am. Chem. Soc.* **2000**, *122*, 178–179. (g) Shin, J. H.; Parkin, G. *Chem. Commun.* **1999**, 887–888. (h) Lee, H.; Desrosiers, P. J.; Guzei, I.; Rheingold, A. L.; Parkin, G. *J. Am. Chem. Soc.* **1998**, *120*, 3255–3256. (i) Wochner, F.; Brintzinger, H. H. *J. Organomet. Chem.* **1986**, *309*, 65–75. (j) Smith, J. A.; Brintzinger, H. H. *J. Organomet. Chem.* **1981**, *218*, 159–167. (k) Dorer, B.; Diebold, J.; Weyand, O.; Brintzinger, H. H. *J. Organomet. Chem.* **1992**, *427*, 245–255. (l) Fendrick, C. M.; Schertz, L. D.; Day, V. W.; Marks, T. J. *Organometallics* **1988**, *7*, 1828–1838.

(4) (a) Siemeling, U. *Chem. Rev.* **2000**, *100*, 1495–1526. (b) Butenschön, H. *Chem. Rev.* **2000**, *100*, 1527–1564. (c) Jutzki, P.; Redeker, T. *Eur. J. Inorg. Chem.* **1998**, 663–674.

(5) (a) Alt, H. G.; Samuel, E. *Chem. Soc. Rev.* **1998**, *27*, 323–329. (b) Repo, T.; Jany, G.; Hakala, K.; Klinga, M.; Polamo, M.; Leskelä; Rieger, B. *J. Organomet. Chem.* **1997**, *549*, 177–186.

(6) O'Connor, J. M.; Casey, C. P. *Chem. Rev.* **1987**, *87*, 307–318.

(7) (a) Rerek, M. E.; Ji, L. N.; Basolo, F. *J. Chem. Soc., Chem. Commun.* **1983**, 1208–1209. (b) Rerek, M. E.; Basolo, F. *J. Am. Chem. Soc.* **1984**, *106*, 5908–5912.

(8) Miyamoto, T. K.; Tsutsui, M.; Chen, L. B. *Chem. Lett.* **1981**, 729–730.

(9) Ready, T. E.; Chien, J. C. W.; Rausch, M. D. *J. Organomet. Chem.* **1999**, *583*, 11–27.

(10) O'Hare, D.; Murphy, V.; Kaltsoyannis, N. *J. Chem. Soc., Dalton Trans.* **1993**, 383–392.

(11) O'Hare, D.; Kakkar, A. K.; Stringer, G.; Taylor, N. J.; Marder, T. B. *J. Organomet. Chem.* **1990**, *394*, 777–794.

(12) O'Hare, D.; Green, J. C.; Marder, T.; Collins, S.; Stringer, G.; Kakkar, A. K.; Kaltsoyannis, N.; Kuhn, A.; Lewis, R.; Mehnert, C.; Scott, P.; Kurmoo, M.; Pugh, S. *Organometallics* **1992**, *11*, 48–55.

(13) O'Hare, D.; Murphy, V.; Diamond, G. M.; Arnold, P.; Mountford, P. *Organometallics* **1994**, *13*, 4689–4694.

(14) Green, M.; McGrath, T. D.; Thomas, R. L.; Walker, A. P. *J. Organomet. Chem.* **1997**, *532*, 61–70.

(15) Herrmann, W. A.; Geisberger, M. R.; Kühn, F. E.; Artus, G. R. J.; Herdtweck, E. *Z. Anorg. Allg. Chem.* **1997**, *623*, 1229–1236.

(16) Kakkar, A. K.; Taylor, N. J.; Marder, T. B.; Shen, J. K.; Hallinan, N.; Basolo, F. *Inorg. Chim. Acta* **1992**, *198–200*, 219–231.

(17) Kakkar, A. K.; Jones, S. F.; Taylor, N. J.; Collins, S.; Marder, T. B. *J. Chem. Soc., Chem. Commun.* **1989**, 1454–1456.

(18) Kakkar, A. K.; Stringer, G.; Taylor, N. J.; Marder, T. B. *Can. J. Chem.* **1995**, *73*, 981–988.

(19) Frankom, T. M.; Green, J. C.; Nagy, A.; Kakkar, A. K.; Marder, T. B. *Organometallics* **1993**, *12*, 3688–3697.

(20) (a) Mantovani, L.; Cecon, A.; Gambaro, A.; Santi, S.; Ganis, P.; Venzo, A. *Organometallics* **1997**, *16*, 2682–2690. (b) Bonifaci, C.; Cecon, A.; Gambaro, A.; Ganis, P.; Mantovani, L.; Santi, S.; Venzo, A. *J. Organomet. Chem.* **1994**, *475*, 267–276.

(21) Tsutsui, M.; Chen, L. B.; Bergbreiter, D. E.; Miyamoto, T. K. *J. Am. Chem. Soc.* **1982**, *104*, 855–856.

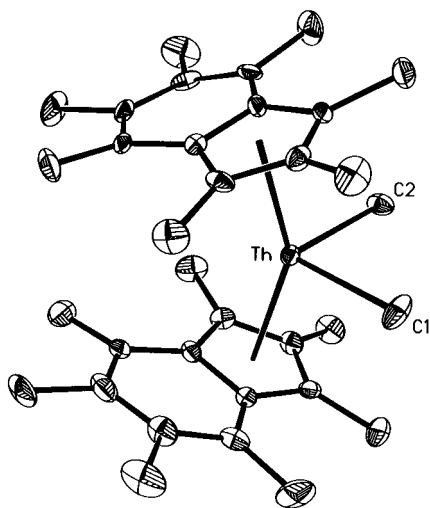
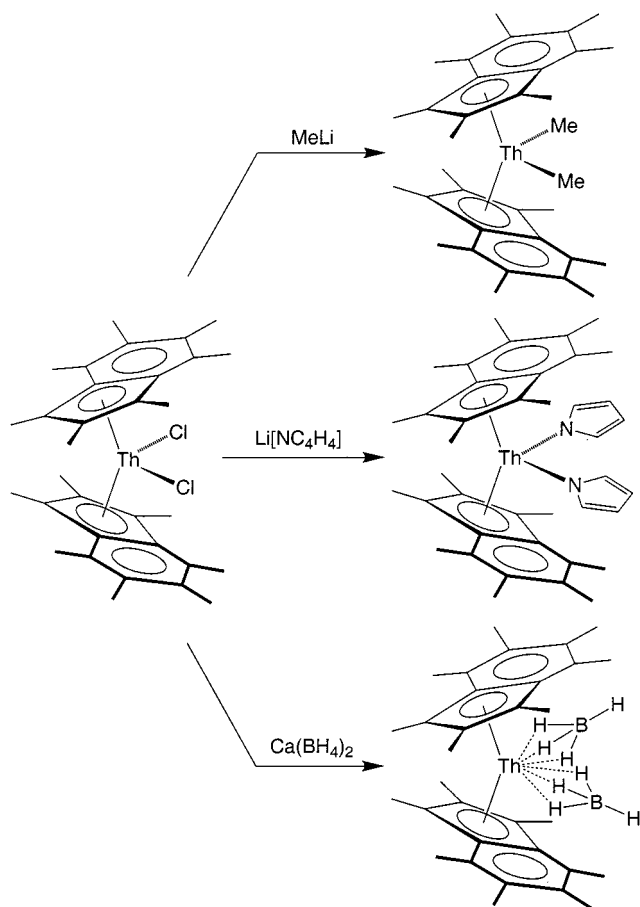


Figure 3. Molecular structure of $\text{Ind}^*_2\text{ThMe}_2$. Selected bond lengths (Å) and angles (deg): $\text{Th}-\text{C}(1) = 2.48(2)$, $\text{Th}-\text{C}(2) = 2.47(2)$; $\text{C}(1)-\text{Th}-\text{C}(2) = 88.2(6)$.

Scheme 2



^1H and ^{13}C NMR spectra,²⁸ respectively, and the complex has been structurally characterized by X-ray diffraction (Figure 3). The average $\text{Th}-\text{CH}_3$ bond length is 2.48 Å and compares favorably with the mean value of 2.45 Å for other structurally characterized complexes listed in the Cambridge Structural Database.²⁷ Amide derivatives may be obtained by the reactions of Ind^*_2 -

(28) For comparison, the ^{13}C NMR signal for $\text{Cp}^*_2\text{ThMe}_2$ is observed at 68.0 and 68.4 ppm in the solution and solid state, respectively. See ref 24c and: Toscano, P. J.; Marks, T. J. *J. Am. Chem. Soc.* **1985**, *107*, 653–659.

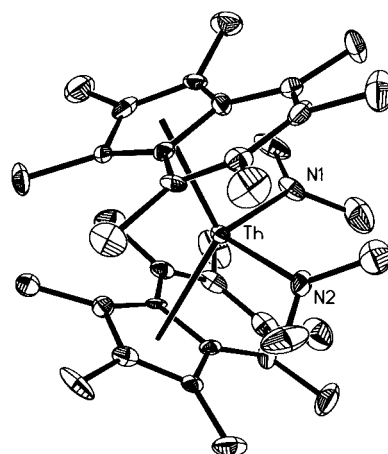


Figure 4. Molecular structure of $\text{Ind}^*_2\text{Th}(\text{NMe}_2)_2$. Selected bond lengths (Å) and angles (deg): $\text{Th}-\text{N}(1) = 2.26(2)$, $\text{Th}-\text{N}(2) = 2.24(2)$; $\text{N}(1)-\text{Th}-\text{N}(2) = 102.4(7)$.

Scheme 3

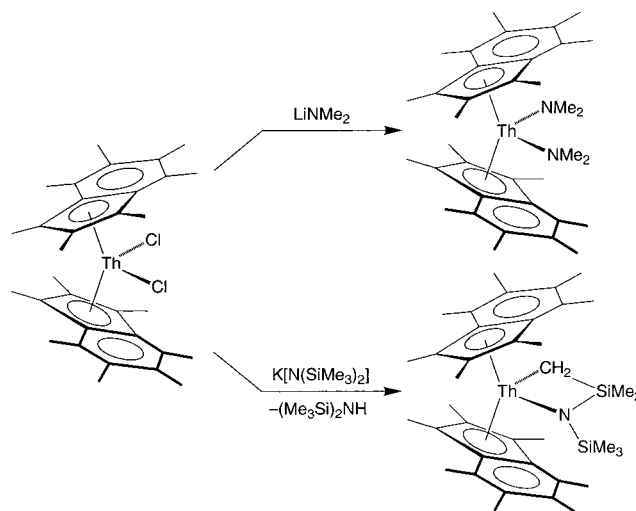


Table 1. $[\text{ThX}_2]$ Bond Lengths and Angles for $\text{Ind}^*_2\text{ThX}_2$ Complexes

	$d(\text{Th}-\text{X})/\text{Å}$	$\text{X}-\text{Th}-\text{X}/\text{deg}$
$\text{Ind}^*_2\text{ThCl}_2$	2.62	91.8
$\text{Ind}^*_2\text{ThMe}_2$	2.48	88.2
$\text{Ind}^*_2\text{Th}(\text{NMe}_2)_2$	2.25	102.4
$\text{Ind}^*_2\text{Th}[\text{CH}_2\text{SiMe}_2\text{N}(\text{SiMe}_3)]$	2.29, 2.44	70.9

ThCl_2 with LiNMe_2 and LiNC_4H_4 to yield $\text{Ind}^*_2\text{Th}(\text{NMe}_2)_2$ and $\text{Ind}^*_2\text{Th}(\text{NC}_4\text{H}_4)_2$,²⁹ respectively (Schemes 2 and 3). The molecular structure of $\text{Ind}^*_2\text{Th}(\text{NMe}_2)_2$ is shown in Figure 4, a significant feature of which is the planarity of both NMe_2 ligands. Furthermore, the two NMe_2 ligands lie close to the $[\text{ThN}_2]$ plane,³⁰ such that the nonbonded interactions between the methyl groups result in a $\text{N}-\text{Th}-\text{N}$ bond angle ($102.4(7)^\circ$) that is significantly greater than the corresponding $\text{X}-\text{Th}-\text{X}$ angles in $\text{Ind}^*_2\text{ThCl}_2$ and $\text{Ind}^*_2\text{ThMe}_2$ (Table 1). Although there are no structurally characterized $\text{Th}-\text{NMe}_2$ complexes listed in the Cambridge Structural Database, the average $\text{Th}-\text{N}$ bond length in Ind^*_2 -

(29) Although there are many reports of amide complexes of thorium, we are aware of only one report of an actinide pyrrolyl complex, namely $\text{U}[\text{NC}_4\text{H}_2\text{Me}_2]_4$. See: Marks, T. J.; Kolb, J. R. *J. Organomet. Chem.* **1974**, *82*, C35–C39.

(30) Each NMe_2 ligand is rotated by ca. 21° out of the $[\text{ThN}_2]$ plane.

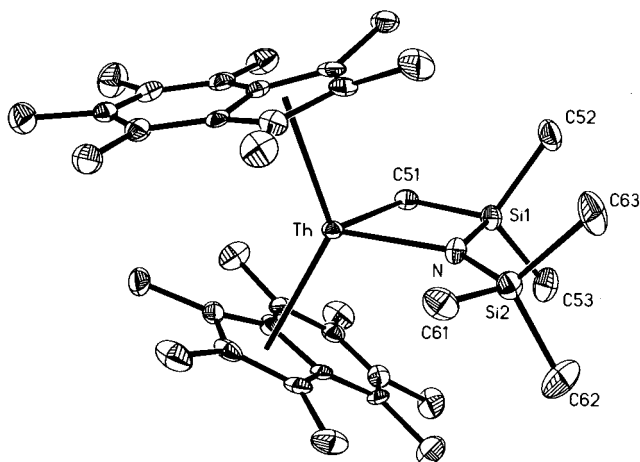


Figure 5. Molecular structure of $\text{Ind}^*_2\text{Th}[\eta^2\text{-CH}_2\text{SiMe}_2\text{-NSiMe}_3]$. Selected bond lengths (Å) and angles (deg): Th–N = 2.286(6), Th–C(51) = 2.438(9), Si(1)–C(51) = 1.853(9), Si(1)–N = 1.757(7); N–Th–C(51) = 70.9(3), Si(1)–N–Th = 98.9(3), N–Si(1)–C(51) = 98.8(4), Si(1)–C(51)–Th = 91.1(3).

ThNMe_2 is 2.25 Å, comparable to the mean value of 2.31 Å for the mixed amide $[(\text{Me}_3\text{Si})_2\text{N}]_2\text{Th}(\text{NMePh})_2$.³¹ Both the planarity at nitrogen and the observation that the Th–NMe₂ bond is 0.23 Å shorter than the average Th–CH₃ bond length (2.48 Å) in $\text{Ind}^*_2\text{ThMe}_2$ indicate that there is nitrogen π -donation to thorium.³² In contrast to forming a simple $\text{Ind}^*_2\text{Th}[\text{N}(\text{SiMe}_3)_2]$ derivative, the reaction of $\text{Ind}^*_2\text{ThCl}_2$ with $\text{K}[\text{N}(\text{SiMe}_3)_2]$ yields the metallacycle complex $\text{Ind}^*_2\text{Th}(\eta^2\text{-CH}_2\text{SiMe}_2\text{NSiMe}_3)$, presumably via elimination of $(\text{Me}_3\text{Si})_2\text{NH}$ (Scheme 3). The first example of a thorium complex containing this four-membered moiety, namely $[(\text{Me}_3\text{Si})_2\text{N}]_2\text{Th}(\eta^2\text{-CH}_2\text{SiMe}_2\text{NSiMe}_3)$, was reported by Andersen.³³ The latter complex may be synthesized by several methods, one of which involves the reaction of $\text{ThBr}_4(\text{THF})_2$ with $\text{K}[\text{N}(\text{SiMe}_3)_2]$.^{34,35} The molecular structure of $\text{Ind}^*_2\text{Th}(\eta^2\text{-CH}_2\text{SiMe}_2\text{NSiMe}_3)$ has been determined by X-ray diffraction, as illustrated in Figure 5. The Th–N (2.286(6) Å) and Th–C (2.438(9) Å) bond lengths associated with the $\eta^2\text{-CH}_2\text{SiMe}_2\text{NSiMe}_3$ ligand are comparable to the respective unconstrained values for $\text{Ind}^*_2\text{Th}(\text{NMe}_2)_2$ (2.25 Å) and $\text{Ind}^*_2\text{ThMe}_2$ (2.48 Å). The N–Th–C bond angle (70.9(3)°) is, nevertheless, smaller than the corresponding values for $\text{Ind}^*_2\text{ThCl}_2$, $\text{Ind}^*_2\text{ThMe}_2$, and $\text{Ind}^*_2\text{Th}(\text{NMe}_2)_2$, due to the constraints imposed by the four-membered ring (Table 1).

Finally, $\text{Ind}^*_2\text{ThCl}_2$ is a suitable precursor for the borohydride complex $\text{Ind}^*_2\text{Th}(\eta^3\text{-H}_3\text{BH})_2$ by reaction with $\text{Ca}(\text{BH}_4)_2 \cdot 2\text{THF}$ (Scheme 2).³⁶ The molecular struc-

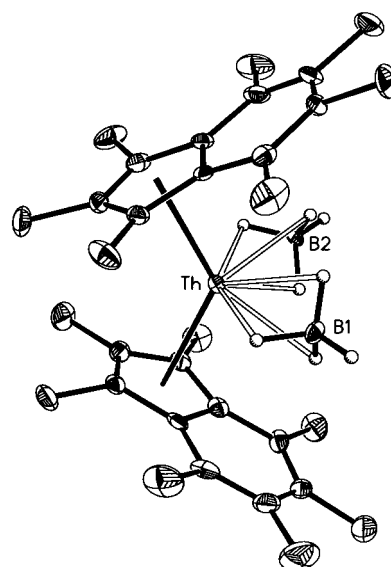


Figure 6. Molecular structure of $\text{Ind}^*_2\text{Th}(\eta^3\text{-H}_3\text{BH})_2$. The hydrogen atoms attached to boron were not located but are placed in calculated positions. Selected bond lengths (Å) and angles (deg): Th···B(1) = 2.624(3), Th···B(2) = 2.618(7); B(1)–Th–B(2) = 98.6(2).

ture of $\text{Ind}^*_2\text{Th}(\eta^3\text{-H}_3\text{BH})_2$ has been determined by X-ray diffraction (Figure 6).³⁷ Although the borohydride hydrogen atoms were not located and refined, the Th···B separation of 2.62 Å is more consistent with tridentate, rather than bidentate, coordination. Specifically, actinide···B separations are typically ca. 2.5 and 2.9 Å for tridentate and bidentate borohydride coordination, respectively.³⁸ For example, the Th···B separations for the tridentate borohydride ligands in $[(\text{Me}_3\text{Si})_2\text{N}]_3\text{Th}(\eta^3\text{-H}_3\text{BH})$ is 2.61 Å,³⁹ while the average Th···B separations for the tridentate methylborohydride ligands in $\text{Th}(\text{BH}_3\text{Me})_4$, $[\text{Th}(\text{BH}_3\text{Me})_4(\text{THF})]_2$, and $[\text{Th}(\text{BH}_3\text{Me})_4]_2(\text{OEt}_2)$ is ca. 2.57 Å.^{40,41}

Further support for tridentate coordination of the BH_4 ligands in $\text{Ind}^*_2\text{Th}(\eta^3\text{-H}_3\text{BH})_2$ is provided by IR spectroscopy and comparison with the IR spectrum of $\text{Ind}_2\text{Th}(\eta^3\text{-H}_3\text{BH})_2$.⁴² Thus, $\text{Ind}^*_2\text{Th}(\eta^3\text{-H}_3\text{BH})_2$ is characterized by a terminal B–H stretch at 2460 cm^{-1} , bridging B–H

(31) Barnhart, D. M.; Clark, D. L.; Grumbine, S. K.; Watkin, J. G. *Inorg. Chem.* **1995**, *34*, 1695–1699.

(32) Chisholm has noted that a M–NR₂ bond length that is considerably shorter than a related M–CH₂R bond length by more than 0.1 Å (the difference between the covalent radii of a sp³-hybridized carbon atom, 0.77 Å, and that of a sp²-hybridized nitrogen atom, 0.67 Å) is a good indication of π -donation in the former. See: Chisholm, M. H.; Tan, L.-S.; Huffman, J. C. *J. Am. Chem. Soc.* **1982**, *104*, 4879–4884.

(33) Simpson, S. J.; Turner, H. W.; Andersen, R. A. *Inorg. Chem.* **1981**, *20*, 2991–2995.

(34) Clark, D. L.; Frankcom, T. M.; Miller, M. M.; Watkin, J. G. *Inorg. Chem.* **1992**, *31*, 1628–1633.

(35) A related phosphide complex, $\text{Cp}^*_2\text{Th}[\text{CH}_2\text{SiMe}_2\text{P}(\text{SiMe}_3)]$, has been reported.^{24g}

(36) The reaction of $\text{Ind}^*_2\text{ThCl}_2$ with KBH_4 was observed to be slower than that with $\text{Ca}(\text{BH}_4)_2$. For other applications of $\text{M}(\text{BH}_4)_2$ (M = Ca, Sr, Ba), see: (a) Noth, H.; Wiberg, E.; Winter, L. P. *Z. Anorg. Allg. Chem.* **1971**, *386*, 73–86. (b) Makhaev, V. D.; Borisov, A. P.; Lobkovskii, E. B.; Semenenko, K. N. *Izv. Akad. Nauk SSSR, Ser. Khim.* **1980**, *11*, 2614–2617. (c) Kedrova, N. S.; Konoplev, V. N.; Maltseva, N. N.; *Zh. Neorg. Khim.* **1976**, *21*, 2270–2272.

(37) The small atomic displacement parameter of the boron may be a consequence of cocrystallization with a small quantity of $\text{Ind}^*_2\text{ThCl}_2$. Specifically, the mean Th–Cl bond length (2.62 Å) is identical with the Th···B distance (2.62 Å), and so both Cl and B would occupy the same position. The excess electron density provided by the chlorine contaminant would cause the displacement atom to be smaller when refined as boron. See: (a) Parkin, G. *Chem. Rev.* **1993**, *93*, 887–911. (b) Parkin, G. *Acc. Chem. Res.* **1992**, *25*, 455–460.

(38) (a) Marks, T. J.; Kolb, J. R. *Chem. Rev.* **1977**, *77*, 263–293. (b) Ephritikhine, M. *Chem. Rev.* **1997**, *97*, 2193–2242.

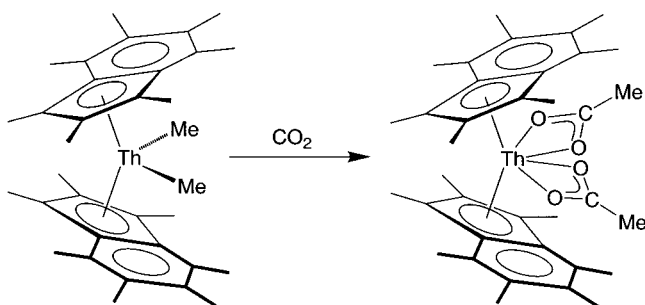
(39) Turner, H. W.; Andersen, R. A.; Zalkin, A.; Templeton, D. H. *Inorg. Chem.* **1979**, *18*, 1221–1224.

(40) (a) Shinomoto, R.; Brennan, J. G.; Edelstein, N. M.; Zalkin, A. *Inorg. Chem.* **1985**, *24*, 2896–2900. (b) Shinomoto, R.; Gamp, E.; Edelstein, N. M.; Templeton, D. H.; Zalkin, A. *Inorg. Chem.* **1983**, *22*, 2351–2355.

(41) For further comparison, the U···B separation in $\text{Cp}^*_2\text{U}(\eta^3\text{-H}_3\text{BH})_2$ is 2.58 Å. See: Gradoz, P.; Baudry, D.; Ephritikhine, M.; Lance, M.; Nierlich, M.; Vigner, J. *J. Organomet. Chem.* **1994**, *466*, 107–118.

(42) Bettonville, S.; Goffart, J. *J. Organomet. Chem.* **1988**, *356*, 297–305.

Scheme 4



stretches at 2224 and 2106 cm^{-1} , and a strong bridge deformation band at 1175 cm^{-1} , which are comparable to the respective values for $\text{Ind}_2\text{Th}(\eta^3\text{-H}_3\text{BH})_2$: 2480, 2220, 2152, and 1182 cm^{-1} .⁴² Identification of the $\eta^3\text{-H}_3\text{BH}$ coordination mode for these complexes is based on the fact that this coordination mode is typically characterized by a sharp terminal B–H stretch in the range 2450–2600 cm^{-1} , while the bridging B–H stretches are observed as two absorptions in the range 2100–2200 cm^{-1} (which are sometimes not resolved); bidentate coordination, on the other hand, is characterized by four bands in the regions 2400–2600, 1650–2150, 1300–1500, and 1100–1200 cm^{-1} .^{38,43} Furthermore, a principal feature which distinguishes tridentate from bidentate coordination is the relative intensities of the absorptions for the B–H_t and B–H_b groups: for tridentate coordination, the combined B–H_b absorptions are more intense than the B–H_t absorption, whereas the reverse is generally observed for bidentate coordination.³⁸

$\text{Ind}^*_2\text{ThMe}_2$ undergoes several insertion reactions. For example, $\text{Ind}^*_2\text{ThMe}_2$ reacts rapidly with CO_2 to yield the acetate complex $\text{Ind}^*_2\text{Th}(\eta^2\text{-O}_2\text{CMe})_2$ (Scheme 4). IR spectroscopy suggests that the acetate ligands are coordinated in a bidentate terminal manner. Specifically, the difference between the antisymmetric and symmetric $[\text{CO}_2]$ stretches is typically $<150 \text{ cm}^{-1}$ for bidentate coordination modes and $>150 \text{ cm}^{-1}$ for monodentate coordination modes.^{44–46} Thus, with a difference of 44 cm^{-1} for $\text{Ind}^*_2\text{Th}(\eta^2\text{-O}_2\text{CMe})_2$, the acetate coordination mode may be identified as bidentate. Insertion of CO_2 into metal–alkyl bonds to give acetate complexes is well-precedented⁴⁷ and includes the formation of $\text{Cp}^*_2\text{Th}(\text{O}_2\text{CMe})_2$ from $\text{Cp}^*_2\text{ThMe}_2$.⁴⁸ $\text{Ind}^*_2\text{ThMe}_2$ likewise undergoes an insertion reaction with CS_2 to give $\text{Ind}^*_2\text{Th}(\text{S}_2\text{CMe})\text{Me}$. Although $\text{Ind}^*_2\text{Th}(\text{S}_2\text{CMe})\text{Me}$ was not isolated in pure form, it is characterized by ^1H NMR spectroscopic signals at δ 2.63 and 0.06 attributable to the S_2CMe and ThMe groups, respectively. The amide

(43) For a caution concerning the use of IR spectroscopy to identify borohydride coordination modes, see: Corey, E. J.; Cooper, N. J.; Canning, W. M.; Lipscomb, W. N.; Koetzle, T. F. *Inorg. Chem.* **1982**, *21*, 192–199.

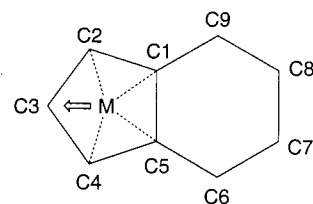
(44) Deacon, G. B.; Phillips, R. J. *Coord. Chem. Rev.* **1980**, *33*, 227–250.

(45) Nakamoto, K. *Infrared and Raman Spectra of Inorganic and Coordination Compounds, Part B: Applications in Coordination, Organometallic, and Bioinorganic Chemistry*; Wiley-Interscience: New York, 1997; pp 271–273.

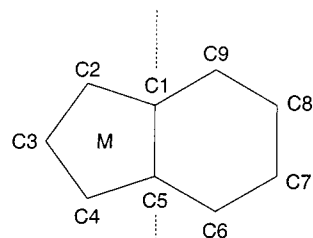
(46) Bridging carboxylate ligands have differences of $>120\text{--}200 \text{ cm}^{-1}$.

(47) Darenbourg, D. J.; Kudaroski, R. A. *Adv. Organomet. Chem.* **1983**, *22*, 129–168.

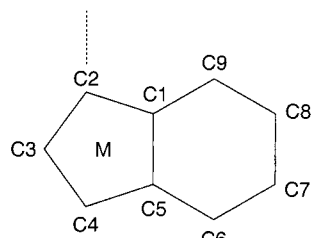
(48) Moloy, K. G.; Marks, T. J. *Inorg. Chim. Acta* **1985**, *110*, 127–131.



$$\Delta_{M-C} = 0.5[M-C1 + M-C5] - 0.5[M-C2 + M-C4]$$



FA = angle between [C1, C2, C3, C4, C5] and [C1, C5, C6, C7, C8, C9]



HA = angle between [C2, C3, C4] and [C1, C2, C4, C5]

Figure 7. Distortion parameters for metal–indenyl bonding.

complex $\text{Ind}^*_2\text{Th}(\text{NMe}_2)_2$ also undergoes an insertion reaction with CO_2 to yield the carbamate complex $\text{Ind}^*_2\text{Th}(\text{O}_2\text{CNMe}_2)_2$, which has been characterized by ^1H NMR spectroscopy. Support for the formulation of $\text{Ind}^*_2\text{Th}(\text{O}_2\text{CNMe}_2)_2$ is provided by analogy to other actinide carbamate derivatives that have been prepared by this method. For example, (i) $\text{Cp}_2\text{U}(\text{NET}_2)_2$ reacts with CO_2 to give $\text{Cp}_2\text{U}(\text{O}_2\text{CNET}_2)_2$,⁴⁹ (ii) $\text{M}(\text{NR}_2)_4$ reacts with CO_2 to give $\text{M}(\text{O}_2\text{CNR}_2)_4$ ($\text{M} = \text{Th}, \text{U}; \text{R} = \text{Me}, \text{Et}$),⁵⁰ and (iii) UCl_4 reacts with R_2NH and CO_2 to yield $\text{U}(\text{O}_2\text{-CNR}_2)_4$ ($\text{R} = \text{Me}, \text{Et}$).⁵¹

Structures of Bis(permethylindenyl)thorium Complexes. An important aspect of the structure of the bis(permethylindenyl)thorium complexes $\text{Ind}^*_2\text{ThX}_2$ is concerned with the coordination mode of the Ind^* ligands. Distortions in metal–indenyl bonding have been previously classified according to three parameters (see Figure 7):^{11,52,53} (i) the slip parameter (Δ_{M-C}), which is defined as the difference between the average distance from the metal center to the two carbons shared by both

(49) Arduini, A. L.; Jamerson, J. D.; Takats, J. *Inorg. Chem.* **1981**, *20*, 2474–2479.

(50) Bagnall, K. W.; Yanir, E. *J. Inorg. Nucl. Chem.* **1974**, *36*, 777–779.

(51) Calderazzo, F.; dell'Amico, G.; Netti, R.; Pasquali, M. *Inorg. Chem.* **1978**, *17*, 471–473.

(52) Cadierno, V.; Diez, J.; Gamasa, M. P.; Gimeno, J.; Lastra, E. *Coord. Chem. Rev.* **1999**, *193–195*, 147–205.

(53) It should be noted that other definitions for defining cyclopentadienyl and indenyl distortions have been introduced. See, for example: (a) Faller, J. W.; Crabtree, R. H.; Habib, A. *Organometallics* **1985**, *4*, 929–935. (b) Grimmond, B. J.; Corey, J. Y.; Rath, N. P. *Organometallics* **1999**, *18*, 404–412.

Table 2. Structural Distortions in {Ind*₂M} Complexes

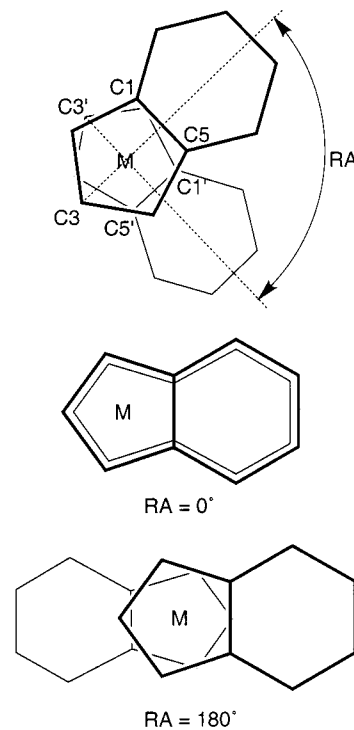
	$d(M-C_{av})/\text{\AA}$	$\Delta_{M-C}/\text{\AA}$	FA/deg	HA/deg	RA/deg	TA/deg	OA/deg
Ind* ₂ ThCl ₂	2.79	-0.06	4.2	2.8	85.4	105.6	7.0
Ind* ₂ ThMe ₂	2.81	0.08	4.2	1.8	84.0	103.6	4.7
Ind* ₂ ThCl(μ -Cl) ₂ Li(tmeda)	2.84	0.05	7.8	5.2	88.0	78.9	73.4
Ind* ₂ Th[CH ₂ SiMe ₂ N(SiMe ₃)]	2.86	0.06	7.2	4.0	108.5	97.4	80.5
Ind* ₂ Th(NMe ₂) ₂	2.88	-0.02	6.2	3.0	94.7	112.7	172.2
Ind* ₂ Th(η^3 -H ₃ BH) ₂	2.81	0.02	6.2	5.2	37.6	40.1	161.1
Ind* ₂ ZrCl ₂ ^a	2.56	0.04	10.4	9.8	89	101.1	5.0
Ind* ₂ Cr ^a	2.18	0.10	3.6	7.2	180	180	c
[Ind* ₂ Cr] ⁺ ^a	2.21	0.02	2.5	5.1	89	91.5	c
Ind* ₂ Fe ^a	2.07	0.03	4.4	2.5	151	89 ^b	c
[Ind* ₂ Co] ⁺ ^a	2.08	0.07	4.8	4.5	89	91.0	c

^a Data taken from: O'Hare, D.; Murphy, V.; Diamond, G. M.; Arnold, P.; Mountford, P. *Organometallics* **1994**, *13*, 4689–4694. ^b The value of 89° is calculated from the structure listed in the CSD; a value of 98° was listed in the original paper. ^c Not applicable to parallel-ring metallocenes.

the five- and six-membered rings (C(1) and C(5)) and the average distance from the metal to the adjacent carbon atoms (C(2) and C(4)), (ii) the fold angle (FA), which is defined as the angle between the planes of the five-membered (C(1), C(2), C(3), C(4), C(5)) and six-membered (C(1), C(5), C(6), C(7), C(8), C(9)) rings, and (iii) the hinge angle (HA), which is defined as the angle between the planes defined by [C(2), C(3), C(4)] and [C(1), C(2), C(4), C(5)]. The distinction between the fold angle and the hinge angle is that the fold angle describes bending at the C(1)–C(5) ring junction, whereas the hinge angle describes bending along the nonbonded C(2)–C(4) vector.

It is pertinent to compare the structures of these Ind*₂Th(X)(Y) derivatives with those of the zirconocene dichloride Ind*₂ZrCl₂ and other bis(permethyindenyl) metal complexes, as summarized in Table 2.¹³ Examination of the data indicates that the permethyindenyl ligand in all Ind*₂Th(X)(Y) derivatives binds principally with an η^5 -coordination mode, with relatively small slip parameters $|\Delta_{M-C}|_{\text{avg}} \approx 0.05 \text{ \AA}$ (Table 2); for comparison, the range of this geometrical parameter is such that "true" η^5 -coordination modes have been classified as possessing $\Delta_{M-C} \approx 0.03 \text{ \AA}$, with "true" η^3 -coordination modes possessing $\Delta_{M-C} \approx 0.80 \text{ \AA}$.^{16,54} Despite the small slip parameters, the hinge and fold angles for Ind*₂Th(X)(Y) are nonzero, indicating a degree of nonplanarity of the Ind* ligand, which presumably arises from steric repulsions between the proximal methyl groups of the two Ind* ligands. In this regard, the observation that the hinge and fold angles for Ind*₂ThCl₂ are less than the corresponding values for Ind*₂ZrCl₂ is consistent with the greater Th–C bond lengths, which help to minimize steric repulsions between the two Ind* ligands in Ind*₂ThCl₂.

In addition to the η^5 versus η^3 nature of the bonding, another interesting aspect of the structures of Ind*₂Th(X)(Y) concerns the conformational preferences of the indenyl ligands. For simple bis(indenyl)metal complexes of the type Ind₂M, the rotation angle (RA), which is defined as the angle between the planes [M, C(3), midpoint of C(1)–C(5)] and [M, C(3'), midpoint of C(1')–C(5')] (see Figure 8), indicates the extent to which the indenyl ligands are staggered with respect to one another; 0° corresponds to an eclipsed conformation,

**Figure 8.** Rotation angles for bis(indenyl) compounds.

while 180° corresponds to a completely staggered arrangement.¹¹ However, for a bent metallocene of the type Ind₂MX₂, two other factors need to be considered. One factor is concerned with the bending of the metallocene fragment. Specifically, if the two indenyl ligands are not parallel, the rotation angle as defined above¹¹ is no longer equal to the angle which describes the staggering of the rings illustrated in Figure 8. The reason for this is that the angle between the two planes [M, C(3), midpoint of C(1)–C(5)] and [M, C(3'), midpoint of C(1')–C(5')] is solely due to the staggering of the indenyl ligands if they are parallel. However, if the metal is not directly on the axis about which the indenyl ligands are staggered, the rotation angle as defined above is a function of both the staggering of the rings and the degree of bending; i.e., the $C_{\text{pcent}}-M-C_{\text{pcent}}$ angle. Therefore, for bent-metallocene complexes, it is more appropriate to consider the indenyl torsion angle (TA, 0–180°), which is defined as C(3)–C_{pcent}–C(3')–C(3'). It should be noted that the indenyl torsion angle is identical to the rotation angle for a parallel-ring

(54) It is notable that η^1 -coordination of the permethyindenyl ligand is known for a tin complex, (η^1 -Ind*)SnMe₃.¹⁵ See: Herrmann, W. A.; Geisberger, M. R.; Kühn, F. E.; Artus, G. R. J.; Herdtweck, E. *Z. Anorg. Allg. Chem.* **1997**, *623*, 1229–1236.

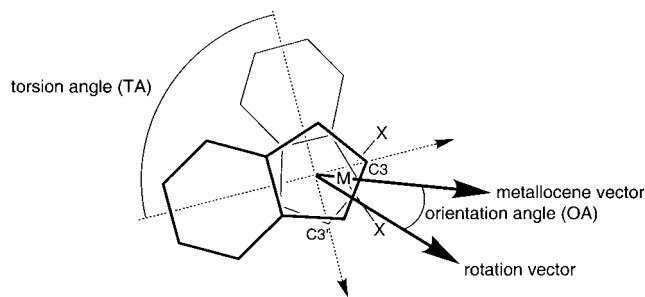


Figure 9. Parameters defining conformations of Ind_2MX_2 complexes: the torsion and orientation angles. The torsion angle is $\text{C}(3)-\text{Cp}'_{\text{cent}}-\text{C}(3')$. The metalocene vector corresponds to the pseudo- C_2 axis of the $[\text{Ind}_2\text{M}]$ fragment, while the rotation vector bisects the torsion angle when projected into the MX_2 plane. The orientation angle is that between the metalocene and rotation vectors.

metallocene and a distinction only arises when the rings bend.

A second factor that needs to be considered for a bent-metallocene complex of the type Ind_2MX_2 is the orientation of the two indenyl ligands relative to the $[\text{MX}_2]$ moiety.^{55,56} The disposition of the indenyl ligands relative to the $[\text{MX}_2]$ moiety may be described by the orientation angle (OA; $0-180^\circ$),⁵⁷ which is defined as the angle between (i) the vector which bisects the torsion angle when projected onto the $[\text{MX}_2]$ plane (rotation vector in Figure 9) and (ii) the metalocene vector, which corresponds to the pseudo- C_2 axis of the $[\text{Ind}_2\text{M}]$ fragment.^{58,59} Thus, whereas the conformation of a parallel-ring Ind_2M complex may be unambiguously defined by a single parameter (RA), that for a bent Ind_2MX_2 complex requires two parameters: the indenyl torsion angle (TA) and the orientation angle (OA).

With respect to the locations of the cyclopentadienyl rings, four idealized classes of conformers may be constructed according to whether (i) the cyclopentadienyl rings are staggered or eclipsed and (ii) one (or both) of the cyclopentadienyl rings is (are) positioned such that an edge is located above the MX_2 group (Figure 10). For each of these four orientations of the cyclopentadienyl groups, it is possible to construct many Ind_2MX_2 conformations according to the dispositions of the two six-membered rings, as illustrated for class I in Figure 11.

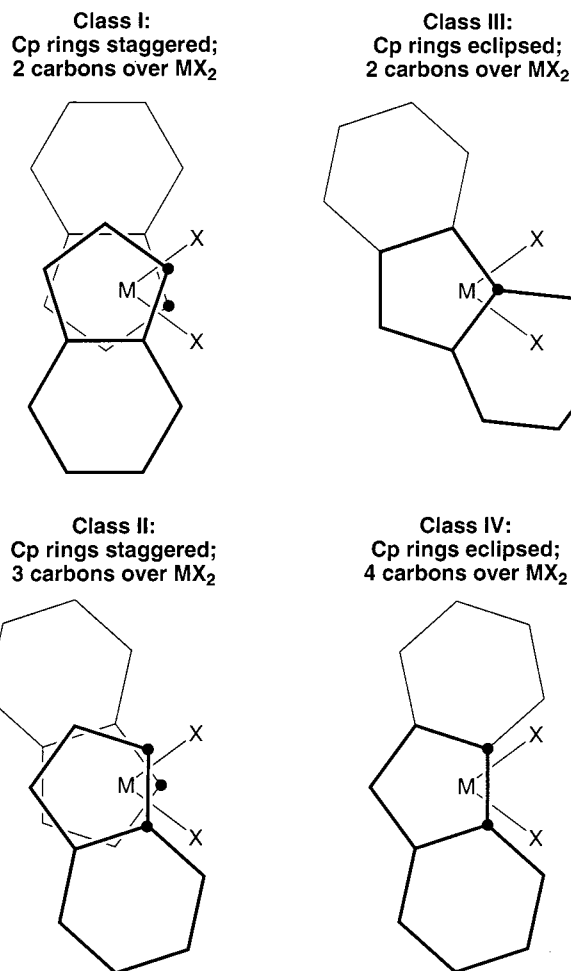


Figure 10. The four basic orientations of the cyclopentadienyl ligands that determine the conformations of Ind_2MX_2 . In each case the six-membered rings are arbitrarily placed in a distal arrangement.

The structures of the thorium complexes reported here belong to classes I, II, and IV (Figure 12). For example, the conformations of $\text{Ind}^*_2\text{ThCl}_2$, $\text{Ind}^*_2\text{ThMe}_2$, $\text{Ind}^*_2\text{Th}(\text{NMe}_2)_2$, and $\text{Ind}^*_2\text{Th}(\eta^2\text{-CH}_2\text{SiMe}_2\text{NSiMe}_3)$ are all staggered (Figure 12) and belong to class I (Figure 10). Despite this similarity, the indenyl torsion angles and orientation angles vary quite dramatically. At one extreme, the dichloride and dimethyl complexes adopt a conformation with C_2 symmetry in which the six-membered rings point away from the Th-X ligands,⁶⁰ with orientation angles close to zero. At the other extreme, the bis(dimethylamido) complex $\text{Ind}^*_2\text{Th}(\text{NMe}_2)_2$ adopts a conformation with C_2 symmetry in which both six-membered rings are located over a Th-NMe_2 bond, with an orientation angle close to 180° .⁶¹ An intermediate class I conformation is observed for $\text{Ind}^*_2\text{Th}(\eta^2\text{-CH}_2\text{SiMe}_2\text{NSiMe}_3)$, in which one of the six-membered rings points away from the Th-N ligands, while the other is located above the Th-C bonds and the orientation angle is close to 90° . $\text{Ind}^*_2\text{ThCl}(\mu\text{-Cl})_2\text{Li}(\text{tmeda})$ exhibits a similar structure to that of Ind^*_2Th

(55) Trnka, T. M.; Bridgewater, B. M.; Parkin, G. Manuscript in preparation.

(56) Torsional isomerism of Ind_2MX_2 complexes has been discussed previously in the literature, but the existence of only three conformers was considered. See: (a) Krüger, C.; Lutz, F.; Nolte, M.; Erker, G.; Aulbach, M. *J. Organomet. Chem.* **1993**, *452*, 79–86. (b) Knickmeier, M.; Erker, G.; Fox, T. *J. Am. Chem. Soc.* **1996**, *118*, 9623–9630. (c) Erker, G.; Aulbach, M.; Knickmeier, M.; Wingbermühle, D.; Krüger, C.; Nolte, M.; Werner, S. *J. Am. Chem. Soc.* **1993**, *115*, 4590–4601. (d) Dreier, T.; Unger, G.; Erker, G.; Wibbeling, B.; Fröhlich, R. *J. Organomet. Chem.* **2001**, *622*, 143–148.

(57) It should be noted that when $\text{TA} = 180^\circ$, two values of OA in the range $0-180^\circ$ exist, which sum to 180° . For convenience, we adopt the smaller value as OA.

(58) The metalocene vector may be conveniently defined as the vector from the midpoint of $\text{Cp}_{\text{cent}}-\text{Cp}'_{\text{cent}}$, i.e. $\{\text{Cp}_{\text{cent}}-\text{cent}'\}$, to the metal.

(59) Operationally, the OA may be calculated as the average of the individual orientation angles for the two indenyl ligands. The individual orientation angle may be defined as the angle between the planes $[\text{C}(3)-\text{Cp}_{\text{cent}}-\{\text{Cp}_{\text{cent}}-\text{cent}'\}]$ and $[\text{Cp}_{\text{cent}}-\text{M}-\text{Cp}'_{\text{cent}}]$. This procedure for calculating OA requires due consideration of the signs of the individual orientation angles: i.e., whether the individual rotation vectors are clockwise or counterclockwise from the metalocene vector.

(60) This conformation is similar to that reported by O'Hare for the zirconium analogue, $\text{Ind}^*_2\text{ZrCl}_2$.¹³

(61) A similar conformation was observed for $\text{Ind}_2\text{ZrMe}_2$. See: Atwood, J. L.; Hunter, W. E.; Hrnčir, D. C.; Samuel, E.; Alt, H.; Rausch, M. *Inorg. Chem.* **1975**, *14*, 1757–1762.

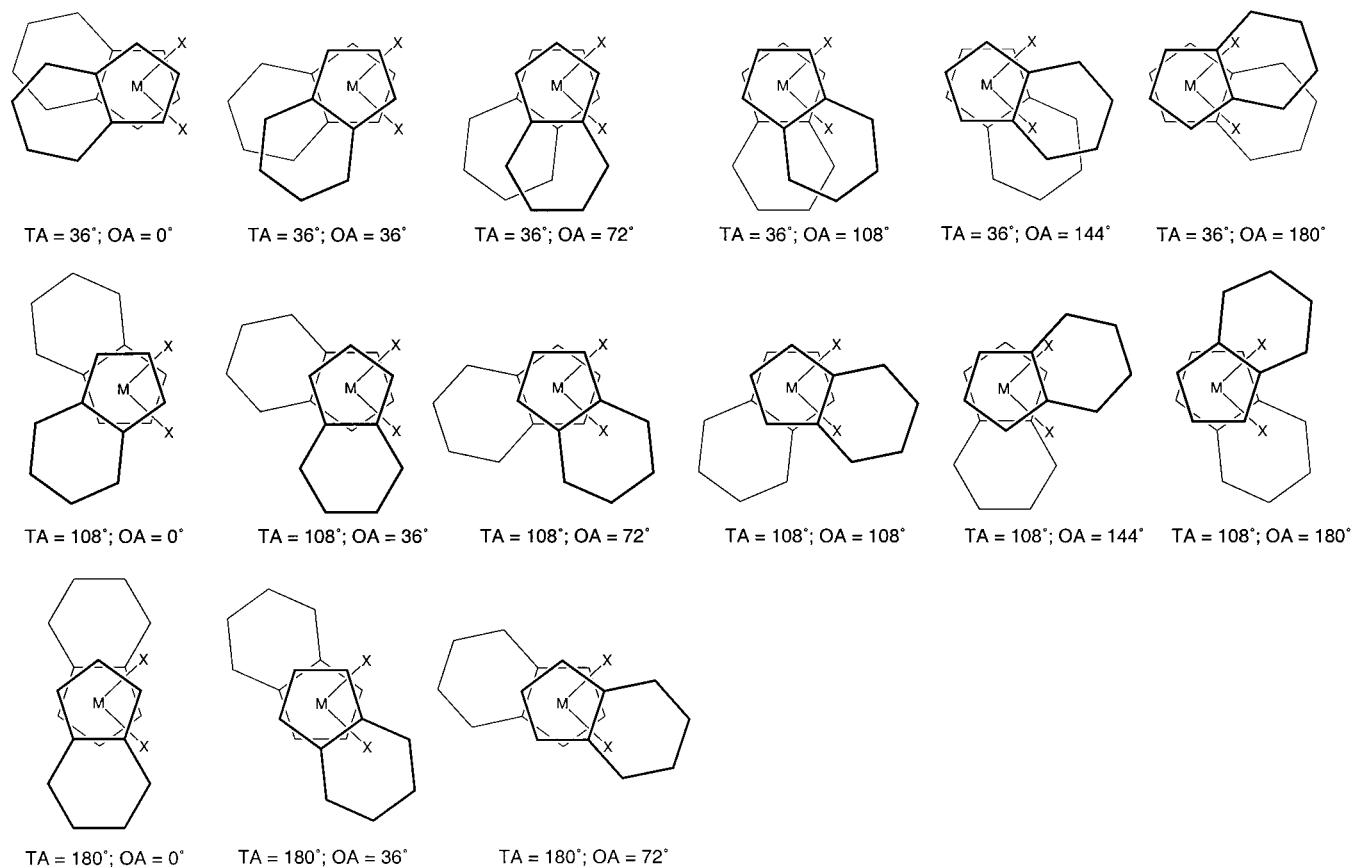


Figure 11. Torsional conformers of Ind_2MX_2 for a class I staggered arrangement of cyclopentadienyl rings.

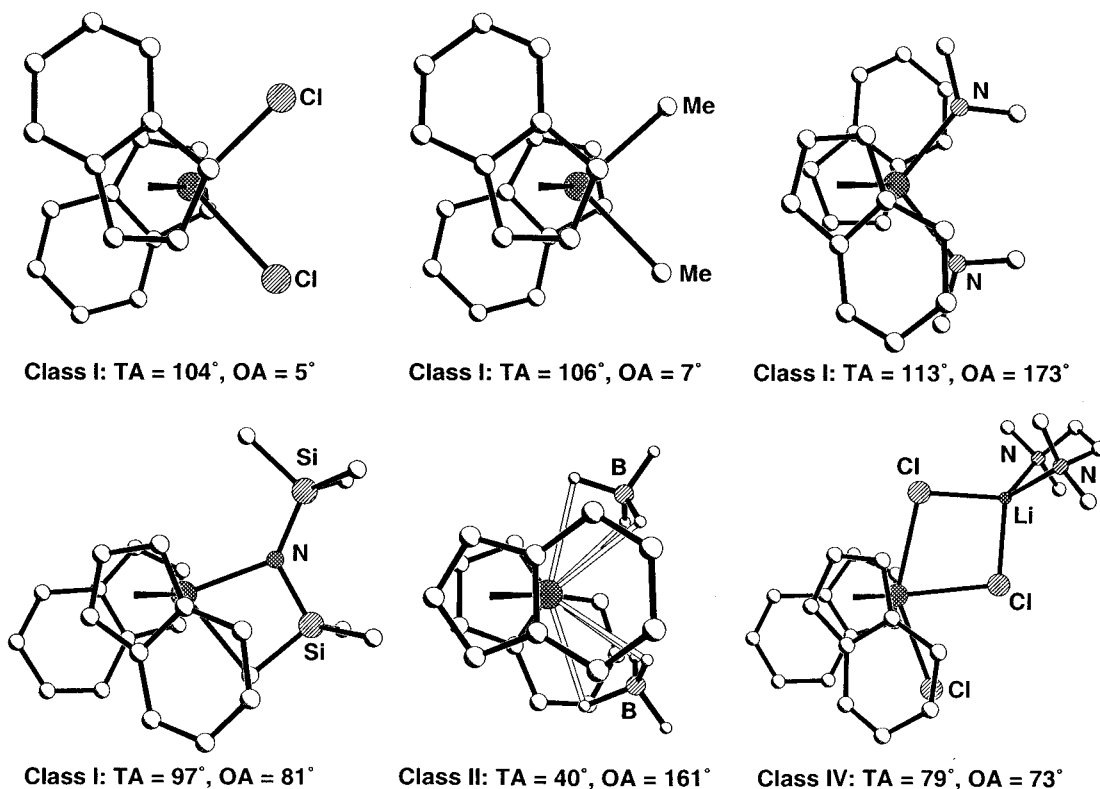


Figure 12. Conformations of $\text{Ind}^*_2\text{ThX}_2$ complexes. Ind^* methyl substituents are omitted for clarity.

($\eta^2\text{-CH}_2\text{SiMe}_2\text{NSiMe}_3$), with the distinction that the indenyl rings of $\text{Ind}^*_2\text{ThCl}(\mu\text{-Cl})_2\text{Li}(\text{tmeda})$ adopt an almost eclipsed class IV conformation. For both $\text{Ind}^*_2\text{-Th}(\eta^2\text{-CH}_2\text{SiMe}_2\text{NSiMe}_3)$ and $\text{Ind}^*_2\text{ThCl}(\mu\text{-Cl})_2\text{Li}(\text{tmeda})$,

the six-membered ring eclipses the Th–X bond of the smaller substituent in order to minimize steric interactions. Thus, it is the Th–C bond that is eclipsed by the six-membered ring in $\text{Ind}^*_2\text{Th}(\eta^2\text{-CH}_2\text{SiMe}_2\text{NSiMe}_3)$

and the terminal Th–Cl bond that is eclipsed in $\text{Ind}^*_2\text{-ThCl}(\mu\text{-Cl})_2\text{Li}(\text{tmeda})$. Finally, the borohydride complex $\text{Ind}^*_2\text{Th}(\eta^3\text{-H}_3\text{BH})_2$ adopts a class II staggered conformation (Figure 10), in which one of the six-membered rings is symmetrically located above both borohydride ligands, while the other is located above only one of the borohydride ligands. As such, this complex has the greatest degree of overlap of the six-membered rings and correspondingly the smallest indenyl torsion angle (40.1°) of all $\text{Ind}^*_2\text{ThX}_2$ derivatives (Figure 12). It is, therefore, evident that the permethyindenyl ligands can adopt a wide variety of conformations in $\text{Ind}^*_2\text{ThX}_2$ complexes.

Experimental Section

General Considerations. All manipulations were performed using a combination of glovebox, high-vacuum, and Schlenk techniques under a nitrogen or argon atmosphere. Solvents were purified and degassed by standard procedures. ^1H and ^{13}C NMR spectra were measured on Varian VXR 200, 300, and 400 spectrometers and a Bruker 500 spectrometer. Chemical shifts are reported in ppm relative to SiMe_4 (δ 0) and were referenced internally with respect to the protio solvent impurity (δ 7.15 for $\text{C}_6\text{D}_5\text{H}$) and the ^{13}C resonances (δ 128.0 for C_6D_6). Coupling constants are given in hertz. IR spectra were recorded as KBr pellets on a Perkin-Elmer Paragon 1000 spectrophotometer, and the data are reported in reciprocal centimeters. Elemental analyses were measured using a Perkin-Elmer 2400 CHN Elemental Analyzer (some analyses differed by $>0.4\%$ of their calculated value). Ind^*Li was prepared as reported previously.¹²

Synthesis of $\text{Ind}^*_2\text{ThCl}_2$. A mixture of Ind^*Li (2.08 g, 9.45 mmol) and ThCl_4 (1.40 g, 3.75 mmol) in toluene (150 mL) was stirred at 120°C for 3 days. The resulting yellow solution was filtered, and the solvent was removed under reduced pressure. The crystalline yellow product was washed with pentane (200 mL) and dried in vacuo (1.83 g, 67%). Anal. Calcd for $\text{C}_{32}\text{H}_{42}\text{ThCl}_2$: C, 52.7; H, 5.8. Found: C, 52.2; H, 6.1. IR data: 2950 (m), 2901 (m), 2862 (m), 1573 (w), 1514 (w), 1445 (s), 1376 (s), 1283 (m), 1165 (w), 1116 (w), 1087 (m), 1057 (m), 1003 (s), 969 (m), 802 (2), 724 (w), 606 (w), 572 (w), 488 (w), 415 (m). ^1H NMR (C_6D_6): 2.45 [s, 4CH₃], 2.33 [s, 4CH₃], 2.18 [s, 4CH₃], 2.13 [s, 2CH₃]. ^{13}C NMR (C_6D_6): 12.8 [q, $^1J_{\text{C-H}} = 127$, $\text{C}_9(\text{CH}_3)_7$], 14.1 [q, $^1J_{\text{C-H}} = 127$, $\text{C}_9(\text{CH}_3)_7$], 16.7 [q, $^1J_{\text{C-H}} = 125$, $\text{C}_9(\text{CH}_3)_7$], 17.7 [q, $^1J_{\text{C-H}} = 126$, $\text{C}_9(\text{CH}_3)_7$], 115.4 [s, $\text{C}_9(\text{CH}_3)_7$], 131.1 [s, $\text{C}_9(\text{CH}_3)_7$], 132.5 [s, $\text{C}_9(\text{CH}_3)_7$], and 140.1 [s, $\text{C}_9(\text{CH}_3)_7$]; one $\text{C}_9(\text{CH}_3)_7$ resonance obscured by C_6D_6 .

Synthesis of $\text{Ind}^*_2\text{ThMe}_2$. A mixture of $\text{Ind}^*_2\text{ThCl}_2$ (0.78 g, 1.07 mmol) and MeLi (0.06 g, 2.73 mmol) in benzene (15 mL) was stirred at room temperature for 10 h. The resulting cloudy yellow solution was filtered, and the filtrate was lyophilized to give $\text{Ind}^*_2\text{ThMe}_2$ as a fluffy, pale yellow solid (0.60 g, 82%). Anal. Calcd for $\text{C}_{34}\text{H}_{48}\text{Th}$: C, 59.3; H, 7.0. Found: C, 58.8; H, 6.9. IR data: 2902 (s), 2857 (s), 2723 (w), 1442 (s), 1378 (s), 1290 (m), 1261 (w), 1093 (s), 1057 (m), 1005 (m), 967 (w), 809 (w), 731 (w), 605 (w). ^1H NMR (C_6D_6): 2.39 [s, 4CH₃], 2.27 [s, 4CH₃], 2.17 [s, 4CH₃], 1.92 [s, 2CH₃], -0.46 [s, 2Th(CH₃)]. ^{13}C NMR (C_6D_6): 11.5 [q, $^1J_{\text{C-H}} = 126$, $\text{C}_9(\text{CH}_3)_7$], 14.2 [q, $^1J_{\text{C-H}} = 127$, $\text{C}_9(\text{CH}_3)_7$], 16.7 [q, $^1J_{\text{C-H}} = 125$, $\text{C}_9(\text{CH}_3)_7$], 17.6 [q, $^1J_{\text{C-H}} = 126$, $\text{C}_9(\text{CH}_3)_7$], 68.4 [q, $^1J_{\text{C-H}} = 113$, 2Th(CH₃)], 109.9 [s, $\text{C}_9(\text{CH}_3)_7$], 126.7 [s, $\text{C}_9(\text{CH}_3)_7$], 129.3 [s, $\text{C}_9(\text{CH}_3)_7$], 129.9 [s, $\text{C}_9(\text{CH}_3)_7$], and 134.7 [s, $\text{C}_9(\text{CH}_3)_7$].

Synthesis of $\text{Ind}^*_2\text{Th}(\text{NC}_4\text{H}_4)_2$. A mixture of $\text{Ind}^*_2\text{ThCl}_2$ (0.35 g, 0.48 mmol) and LiNC_4H_4 (0.11 g, 1.44 mmol) in toluene (25 mL) was stirred at room temperature for 12 h. The resulting cloudy yellow solution was filtered, and the solvent was removed from the filtrate under reduced pressure, giving $\text{Ind}^*_2\text{Th}(\text{NC}_4\text{H}_4)_2$ as a yellow solid (0.32 g, 85%). Anal. Calcd for $\text{C}_{40}\text{H}_{50}\text{N}_2\text{Th}$: C, 60.8; H, 6.4; N, 3.5. Found: C, 59.6; H,

6.2; N, 3.6. IR data: 3096 (w), 2961 (m), 2913 (s), 2865 (s), 2730 (w), 1441 (s), 1379 (m), 1287 (m), 1191 (w), 1066 (s), 1018 (s), 602 (m), 715 (s), 638 (m). ^1H NMR (C_6D_6): 6.72 [s, 4H of 2 NC_4H_4], 6.62 [s, 4H of 2 NC_4H_4], 2.31 [s, 4CH₃], 2.11 [s, 4CH₃], 2.06 [s, 4CH₃], 1.67 [s, 2CH₃]. ^{13}C NMR (C_6D_6): 10.6 [q, $^1J_{\text{C-H}} = 127$, $\text{C}_9(\text{CH}_3)_7$], 13.9 [q, $^1J_{\text{C-H}} = 127$, $\text{C}_9(\text{CH}_3)_7$], 16.7 [q, $^1J_{\text{C-H}} = 126$, $\text{C}_9(\text{CH}_3)_7$], 17.7 [q, $^1J_{\text{C-H}} = 126$, $\text{C}_9(\text{CH}_3)_7$], 110.0 [dd, $^1J_{\text{C-H}} = 167$, $^2J_{\text{C-H}} = 7$, 4C of 2(NC_4H_4)], 115.2 [s, $\text{C}_9(\text{CH}_3)_7$], 123.0 [dd, $^1J_{\text{C-H}} = 174$, $^2J_{\text{C-H}} = 9$, 4C of 2(NC_4H_4)], 131.5 [s, $\text{C}_9(\text{CH}_3)_7$], 133.0 [s, $\text{C}_9(\text{CH}_3)_7$], and 140.0 [s, $\text{C}_9(\text{CH}_3)_7$], one $\text{C}_9(\text{CH}_3)_7$ resonance obscured by C_6D_6 .

Synthesis of $\text{Ind}^*_2\text{Th}(\text{NMe}_2)_2$. A mixture of $\text{Ind}^*_2\text{ThCl}_2$ (0.10 g, 0.14 mmol) and LiNMe_2 (0.02 g, 0.39 mmol) in benzene (10 mL) was stirred at 100°C for 1 day, during which time a white precipitate formed. The reaction mixture was filtered, and the filtrate was lyophilized, giving $\text{Ind}^*_2\text{Th}(\text{NMe}_2)_2$ as a pale yellow powder (0.06 g, 59%). Anal. Calcd for $\text{C}_{36}\text{H}_{54}\text{N}_2\text{Th}$: C, 57.9; H, 7.3; N, 3.8. Found: C, 58.5; H, 7.6; N, 3.9. IR data: 2959 (w), 2913 (m), 2859 (m), 2805 (m), 2750 (m), 1578 (w), 1451 (m), 1424 (m), 1379 (m), 1293 (m), 1229 (m), 1134 (m), 1121 (m), 1089 (m), 1057 (m), 1008 (m), 967 (w), 913 (s), 813 (w), 609 (w). ^1H NMR (C_6D_6): 2.54 [s, 4CH₃], 2.52 [s, 4CH₃], 2.41 [s, 4CH₃], 2.21 [s, 4CH₃], 2.05 [s, 2CH₃]. ^{13}C NMR (C_6D_6): 11.4 [q, $^1J_{\text{C-H}} = 125$, $\text{C}_9(\text{CH}_3)_7$], 15.0 [q, $^1J_{\text{C-H}} = 126$, $\text{C}_9(\text{CH}_3)_7$], 16.6 [q, $^1J_{\text{C-H}} = 125$, $\text{C}_9(\text{CH}_3)_7$], 18.0 [q, $^1J_{\text{C-H}} = 126$, $\text{C}_9(\text{CH}_3)_7$], 40.8 [q, $^1J_{\text{C-H}} = 131$, 2N(CH₃)₂], 111.9 [s, $\text{C}_9(\text{CH}_3)_7$], 122 [s, $\text{C}_9(\text{CH}_3)_7$], 131.3 [s, $\text{C}_9(\text{CH}_3)_7$], and 135.0 [s, $\text{C}_9(\text{CH}_3)_7$]; one $\text{C}_9(\text{CH}_3)_7$ resonance obscured by C_6D_6 .

Synthesis of $\text{Ind}^*_2\text{Th}(\eta^3\text{-H}_3\text{BH})_2$. A mixture of $\text{Ind}^*_2\text{ThCl}_2$ (0.35 g, 0.48 mmol) and $\text{Ca}(\text{BH}_4)_2\cdot 2\text{THF}$ (0.31 g, 1.45 mmol) was stirred in toluene (10 mL) for 3 days at room temperature, after which the cloudy yellow reaction mixture was filtered. The volatile components were removed from the filtrate under reduced pressure to give $\text{Ind}^*_2\text{Th}(\eta^3\text{-H}_3\text{BH})_2$ as a yellow solid (0.21 g, 64%). Anal. Calcd for $\text{C}_{32}\text{H}_{50}\text{B}_2\text{Th}$: C, 55.8; H, 6.2. Found: C, 56.7; H, 7.3. IR data: 2911 (m), 2862 (m), 2725 (m), 2460 (m) [$\nu(\text{B-H}_i)$], 2371 (w), 2283 (w), 2224 (m) [$\nu(\text{B-H}_b)$], 2165 (m), 2106 (m) [$\nu(\text{B-H}_b)$], 1582 (w), 1445 (s), 1381 (s), 1288 (m), 1234 (w), 1175 (s) [B–H_b deformation], 1097 (m), 1062 (m), 1008 (m), 807 (w), 704 (w), 616 (w), 572 (w), 415 (m). ^1H NMR (C_6D_6): 2.84 [q, $^1J_{\text{B-H}} = 82$, 2 BH₄], 2.54 [s, 4CH₃], 2.43 [s, 4CH₃], 2.17 [s, 4CH₃], 1.99 [s, 2CH₃]. ^{13}C NMR (C_6D_6): 12.6 [q, $^1J_{\text{C-H}} = 127$, $\text{C}_9(\text{CH}_3)_7$], 15.3 [q, $^1J_{\text{C-H}} = 127$, $\text{C}_9(\text{CH}_3)_7$], 16.5 [q, $^1J_{\text{C-H}} = 126$, $\text{C}_9(\text{CH}_3)_7$], 17.9 [q, $^1J_{\text{C-H}} = 126$, $\text{C}_9(\text{CH}_3)_7$], 115.1 [s, $\text{C}_9(\text{CH}_3)_7$], 130.8 [s, $\text{C}_9(\text{CH}_3)_7$], 133.2 [s, $\text{C}_9(\text{CH}_3)_7$], 135.7 [s, $\text{C}_9(\text{CH}_3)_7$], and 139.0 [s, $\text{C}_9(\text{CH}_3)_7$].

Synthesis of $\text{Ind}^*_2\text{Th}(\eta^2\text{-CH}_2\text{SiMe}_2\text{NSiMe}_3)$. A mixture of $\text{Ind}^*_2\text{ThCl}_2$ (0.10 g, 0.14 mmol) and $\text{K}[\text{N}(\text{SiMe}_3)_2]$ (0.06 g, 0.30 mmol) was stirred in benzene (1 mL) for 1 day at 90°C , during which time the solution became orange. The reaction mixture was filtered, and the filtrate was lyophilized to give $\text{Ind}^*_2\text{Th}(\eta^2\text{-CH}_2\text{SiMe}_2\text{NSiMe}_3)$ as an orange solid (0.08 g, 72%). Anal. Calcd for $\text{C}_{38}\text{H}_{59}\text{NSi}_2\text{Th}$: C, 55.8; H, 7.3; N, 1.7. Found: C, 55.7; H, 7.4; N, 1.6. IR data: 2956 (m), 2918 (m), 2861 (m), 1629 (m), 1563 (m), 1544 (m), 1526 (m), 1507 (m), 1445 (s), 1379 (s), 1290 (m), 1243 (m), 1185 (m), 1151 (w), 1096 (m), 1005 (m), 947 (m), 835 (m), 757 (w), 662 (w), 592 (m). ^1H NMR (C_6D_6): 2.49 [s, 2CH₃], 2.43 [s, 2CH₃], 2.36 [s, 2CH₃], 2.22 [s, 4CH₃], 2.21 [s, 2CH₃], 1.94 [s, 2CH₃], 0.62 [s, CH₂], 0.37 [s, Si(CH₃)₂], 0.19 [s, 2 Si(CH₃)₃]. ^{13}C NMR (C_6D_6): 5.1 [q, $^1J_{\text{C-H}} = 117$, SiCH₃], 5.8 [q, $^1J_{\text{C-H}} = 116$, SiCH₃], 12.2 [q, $^1J_{\text{C-H}} = 126$, $\text{C}_9(\text{CH}_3)_7$], 14.6 [q, $^1J_{\text{C-H}} = 127$, $\text{C}_9(\text{CH}_3)_7$], 15.4 [q, $^1J_{\text{C-H}} = 126$, $\text{C}_9(\text{CH}_3)_7$], 16.6 [q, $^1J_{\text{C-H}} = 127$, $\text{C}_9(\text{CH}_3)_7$], 17.9 [q, $^1J_{\text{C-H}} = 127$, $\text{C}_9(\text{CH}_3)_7$], 60.8 [t, $^1J_{\text{C-H}} = 126$, CH₂], 111.4 [s, $\text{C}_9(\text{CH}_3)_7$], 111.8 [s, $\text{C}_9(\text{CH}_3)_7$], 126.4 [s, $\text{C}_9(\text{CH}_3)_7$], 129.2 [s, $\text{C}_9(\text{CH}_3)_7$], 129.6 [s, $\text{C}_9(\text{CH}_3)_7$], 132.0 [s, $\text{C}_9(\text{CH}_3)_7$], 132.2 [s, $\text{C}_9(\text{CH}_3)_7$], 135.7 [s, $\text{C}_9(\text{CH}_3)_7$], and 136.8 [s, $\text{C}_9(\text{CH}_3)_7$].

Synthesis of $\text{Ind}^*_2\text{Th}(\eta^2\text{-O}_2\text{CMe})_2$. A solution of $\text{Ind}^*_2\text{ThMe}_2$ (0.10 g, 0.15 mmol) in benzene (2 mL) was treated with CO_2 (1 atm). After 15 min at room temperature, the yellow solution turned orange. The solution was lyophilized to give

Table 3. Crystal Data and Intensity Collection and Refinement Parameters

	Ind* ₂ ThCl ₂	Ind* ₂ ThCl(μ-Cl) ₂ - Li(tmeda)	Ind* ₂ ThMe ₂	Ind* ₂ Th(NMe ₂) ₂	Ind* ₂ Th(η ² -CH ₂ Si- Me ₂ NSiMe ₃)	Ind* ₂ Th(η ³ - H ₃ BH) ₂
lattice	monoclinic	monoclinic	monoclinic	monoclinic	triclinic	triclinic
formula	C ₃₂ H ₄₂ Cl ₂ Th	C ₃₈ H ₅₈ Cl ₃ LiN ₂ Th	C ₃₄ H ₄₈ Th	C ₃₆ H ₅₄ N ₂ Th	C ₃₈ H ₅₆ NSi ₂ Th	C ₃₂ H ₅₀ B ₂ Th
fw	729.60	888.19	688.76	746.85	818.08	688.38
space group	<i>P</i> 2 ₁ / <i>n</i> (No. 14)	<i>P</i> 2 ₁ / <i>c</i> (No. 14)	<i>P</i> 2 ₁ / <i>n</i> (No. 14)	<i>P</i> 2 ₁ / <i>c</i> (No. 14)	<i>P</i> $\bar{1}$ (No. 2)	<i>P</i> $\bar{1}$ (No. 2)
<i>a</i> /Å	14.426(2)	13.472(4)	14.549(3)	10.039(2)	9.212(3)	8.357(3)
<i>b</i> /Å	13.462(2)	14.820(6)	13.457(3)	34.683(6)	11.763(2)	9.296(2)
<i>c</i> /Å	15.284(2)	20.338(9)	15.310(5)	10.143(3)	18.967(3)	21.132(3)
α /deg	90	90	90	90	77.62(1)	98.15(1)
β /deg	99.33(1)	100.78(1)	99.69(2)	112.32(3)	78.90(2)	91.95(1)
γ /deg	90	90	90	90	68.02(2)	112.06(3)
<i>V</i> /Å ³	2929(1)	3989(3)	2955(1)	3267(1)	1847(1)	1499.4(7)
<i>Z</i>	4	4	4	4	2	2
temp (K)	293	293	293	293	293	293
radiation (λ , Å)	0.710 73	0.710 73	0.710 73	0.710 73	0.710 73	0.710 73
ρ (calcd), g cm ⁻³	1.655	1.479	1.548	1.518	1.471	1.525
μ (Mo K α), mm ⁻¹	5.292	3.966	5.066	4.589	4.126	4.990
θ_{\max} , deg	22.5	22.5	22.5	24.0	22.5	22.5
no. of data	3805	5122	3786	5048	4787	3885
no. of parameters	317	407	317	353	380	342
R1	0.0492	0.0656	0.0552	0.0660	0.0468	0.0391
wR2	0.1088	0.1494	0.1248	0.1510	0.0909	0.0942
GOF	1.010	1.049	1.036	1.066	1.060	1.078

Ind*₂Th(η²-O₂CMe)₂ as a pale orange solid (0.09 g, 88%). Anal. Calcd for C₃₆H₄₈O₂Th: C, 55.7; H, 6.2. Found: C, 56.0; H, 6.5. IR data: 2950 (m), 2911 (m), 2872 (m), 2715 (w), 1582 (s) [ν_{as} (CO₂)], 1538 (s) [ν_{s} (CO₂)], 1445 (s), 1381 (s), 1342 (m), 1293 (m), 1092 (m), 1062 (m), 1008 (s), 974 (m), 935 (m), 807 (w), 680 (s), 640 (w), 611 (w), 552 (w), 464 (w), 410 (w). ¹H NMR (C₆D₆): 2.56 [s, 4CH₃], 2.24 [s, 4CH₃], 2.23 [s, 4CH₃], 1.93 [s, 2CH₃], 1.73 [s, 2(O₂CCH₃)]. ¹³C NMR (C₆D₆): 10.7 [q, ¹J_{C-H} = 126, C₉(CH₃)₇], 14.2 [q, ¹J_{C-H} = 126, C₉(CH₃)₇], 16.8 [q, ¹J_{C-H} = 126, C₉(CH₃)₇], 17.4 [q, ¹J_{C-H} = 126, C₉(CH₃)₇], 26.1 [q, ¹J_{C-H} = 128, 2(O₂CCH₃)], 46.6 [s, 2(O₂CCH₃)], 112.8 [s, C₉(CH₃)₇], 130.2 [s, C₉(CH₃)₇], 135.0 [s, C₉(CH₃)₇], and 142.2 [s, C₉(CH₃)₇]; one C₉(CH₃)₇ resonance obscured by C₆D₆.

Reaction of Ind*₂ThMe₂ with CS₂. A solution of Ind*₂-ThMe₂ (ca. 0.01 g) in C₆D₆ (1 mL) was treated with an excess of CS₂. After 12 h at room temperature, the previously yellow solution turned deep orange, and the ¹H NMR spectrum revealed the formation of a new product tentatively identified as Ind*₂Th(S₂CMe)Me. ¹H NMR (C₆D₆): 2.64 [s, S₂CCH₃], 2.44 [s, 2CH₃], 2.42 [s, 2CH₃], 2.32 [s, 2CH₃], 2.27 [s, 2CH₃], 2.22 [s, 2CH₃], 2.20 [s, 2CH₃], 1.98 [s, 2CH₃], 0.06 [3H, s, ThCH₃].

Reaction of Ind*₂ThNMe₂ with CO₂. A solution of Ind*₂-ThNMe₂ (ca. 0.01 g) in C₆D₆ (1 mL) was treated with CO₂ (1 atm). After 12 h at room temperature, the previously yellow solution turned orange, and the ¹H NMR spectrum revealed a new product tentatively identified as Ind*₂Th(O₂CNMe₂)₂. ¹H NMR (C₆D₆): 2.64 [s, 4CH₃], 2.49 [s, 4CH₃], 2.31 [s, 4CH₃], 2.29 [s, 4CH₃], 2.03 [s, 2CH₃].

X-ray Structure Determinations. Crystallographic data were collected using a Siemens P4 diffractometer. Crystal data and data collection and refinement parameters for all complexes are summarized in Table 3. The unit cells were determined by the automatic indexing of 25 centered reflections and confirmed by examination of the axial photographs. Intensity data were collected using graphite-monochromated Mo K α X-radiation ($\lambda = 0.710 73$ Å). Check reflections were measured every 100 reflections, and the data were scaled accordingly and corrected for Lorentz, polarization, and absorption effects. The structures were solved using direct methods and standard difference map techniques and were refined by full-matrix least-squares procedures using SHELX-

TL.⁶² Hydrogen atoms on carbon were included in calculated positions. Atomic coordinates are listed in the Supporting Information.

Summary

In summary, access to bis(permethyindenyl)thorium chemistry has been provided by the synthesis of the dichloride Ind*₂ThCl₂ by reaction of ThCl₄ with Ind*Li. Metathesis of Ind*₂ThCl₂ with MeLi, LiNMe₂, and LiNC₄H₄ yields Ind*₂ThMe₂, Ind*₂Th(NMe₂)₂, and Ind*₂-Th(NC₄H₄)₂, respectively, while reaction with LiN(SiMe₃)₂ yields the metallacycle Ind*₂Th(η²-CH₂SiMe₂-NSiMe₃). The borohydride complex Ind*₂Th(η³-H₃BH)₂, in which the borohydride ligands coordinate in a tridentate manner, has been obtained by reaction of Ind*₂-ThCl₂ with Ca(BH₄)₂. The syntheses of these thorium complexes suggest that the sterically bulky Ind* ligand is a good complement for the large thorium atom. Structural characterization of Ind*₂ThCl₂, Ind*₂ThMe₂, Ind*₂Th(NMe₂)₂, Ind*₂Th(η²-CH₂SiMe₂NSiMe₃), and Ind*₂Th(η³-H₃BH)₂ by X-ray diffraction demonstrates that the indenyl ligands adopt a wide variety of conformations.

Acknowledgment. We thank the U.S. Department of Energy, Office of Basic Energy Sciences (#DE-FG02-93ER14339), for support of this research. T.M.T. also acknowledges the I. I. Rabi Scholar Program at Columbia College for funding (1996–1997). Dr. Matthew Kuchta is thanked for assistance with the preparation of Ind*Li.

Supporting Information Available: Tables of crystallographic data. This material is available free of charge via the Internet at <http://pubs.acs.org>.

OM010233E

(62) Sheldrick, G. M. SHELXTL, An Integrated System for Solving, Refining and Displaying Crystal Structures from Diffraction Data; University of Göttingen, Göttingen, Federal Republic of Germany, 1981.